Mitochondria-mediated anti-proliferation of triple-negative breast cancer cells by Pd(II), Pt(II), and Au(III)- NHC complexes of NCN pincers

Priyanka Sahu,[a] Narayan Ch. Jana,[b] Ananya Das,[c] Nabanita Chatterjee,*[c] Katarzyna Gach-Janczak,[d] Joydev Dinda*[a]

[a]*Department of Chemistry, Utkal University, Vani Vihar, Bhubaneswar-751004, Odisha, India*

[b]*Department of Chemistry, Panskura Banamali College, Panskura RS, West Bengal, 721152, India*

[c]*Department of Receptor Biology and Tumor Metastasis, Chittaranjan National Cancer Institute, Kolkata-700026, West Bengal, India.*

[d]*Department of Biomolecular Chemistry, Medical University of Lodz, Mazowiecka 6/8, 92-215 Lodz, Poland*

[e]*Department of Chemistry, Indian Institute of Technology Bhilai, GEC Campus, Sejbahar, Raipur-492015, Chhattisgarh, India*

Electronic Supplementary Information (ESI)

Table of contents:

Table S1 Summary of key crystallographic data of complexes **2** and **4.**

	2	**4**
Empirical formula	'$C_{23}H_{24.50}ClF_6N_{6.25}O_{0.38}PPd$'	'$C_{24.50}H_{25.25}Au_2Cl_3F_6N_{7.75}P$'
Formula weight	681.31	1073.53
Crystal system	'monoclinic'	'monoclinic'
Space group	C2/c	$P2_1/c$
Temperature (K)	100.00(10)	227.15
Cell dimensions		
a (Å)	24.0097(10)	12.7889(13)
b (Å)	7.9195(3)	20.0668(14)
c (Å)	28.7829(12)	14.4403(12)
α(°)	90	90
β(°)	110.749(5)	115.743(11)
γ(°)	90	90
Volume (Å^3)	5118.0(4)	3338.0(6)
Z	8	4
Density (Mg m^{-3})	1.768	2.136
Absorption coefficient	0.965	9.131
F(000)	2730	2018.0
2Θ range for data collection	5.454-63.918	3.732-59.282
Index ranges	-32<=h<=32,-11<=k<=11,-38<=l<= 42	-16<=h<=16,-24<=k<=24,-17<=l<= 16
Reflections collected	36608	19598
Independent reflections	7478	7079
GOF	1.061	1.067
Final R indices [I>2sigma(I)]	R1= 0.0339, wR2= 0.0834	R1= 0.0600, wR2= 0.1542
R indices (all data)	R1= 0.0371, wR2= 0.0850	R1= 0.0993, wR2= 0.1686

Table S2 Summary of selected bond distances (Å) of complexes **2** and **4**.

2	**Exp.**	**Theo.**	**3**	**Theo.**	**4**	**Exp.**	**Theo.**
Pd(1)-C(10)	1.947(3)	1.965	Pt(1)-C(10)	1.956	Au(1)-C(10)	1.991(11)	2.011
Pd(1)-Cl(1)	2.3510(6)	2.343	Pt(1)-Cl(1)	2.360	Au(1)-Cl(1)	2.302(3)	2.313
Pd(1)-N(1)	2.040(2)	2.070	Pt(1)-N(1)	2.063	Au(1)-N(1)	2.042(8)	2.054
Pd(1)-N(5)	2.068(2)	2.070	Pt(1)-N(5)	2.063	Au(1)-N(5)	2.032(8)	2.054
N(1)-C(1)	1.399(3)	1.398	N(1)-C(1)	1.400	N(1)-C(1)	1.372(14)	1.404
N(1)-C(8)	1.322(3)	1.331	N(1)-C(8)	1.335	N(1)-C(7)	1.356(13)	1.348
N(5)-C(14)	1.330(3)	1.331	N(5)-C(14)	1.335	N(5)-C(14)	1.338(14)	1.348
N(5)-C(15)	1.404(3)	1.398	N(5)-C(15)	1.400	N(5)-C(15)	1.405(13)	1.404
N(3)-C(10)	1.341(3)	1.349	N(3)-C(10)	1.353	N(3)-C(10)	1.286(13)	1.340
N(4)-C(10)	1.341(3)	1.349	N(4)-C(10)	1.353	N(4)-C(10)	1.333(14)	1.340

Table S3 Summary of selected bond angles (°) of complexes **2** and **4**.

2	**Exp.**	**Theo.**	**3**	**Theo.**	**4**	**Exp.**	**Theo.**
C(10)-Pd(1)-Cl(1)	174.11(8)	180.0	C(10)-Pt(1)-Cl(1)	180.00	C(10)-Au(1)-Cl(1)	178.8(3)	180.0
N(1)-Pd(1)-N(5)	173.50(9)	172.2	N(1)- Pt(1)-N(5)	173.32	N(1)-Au(1)-N(5)	173.8(4)	172.6
C(10)-Pd(1)-N(1)	86.43(10)	86.1	C(10)- Pt(1)-N(1)	86.66	C(10)-Au(1)-N(1)	87.3(4)	86.3
C(10)-Pd(1)-N(5)	87.74(10)	86.1	C(10)- Pt(1)-N(5)	86.66	C(10)-Au(1)-N(5)	86.6(4)	86.3
N(1)-Pd(1)-Cl(1)	90.74(7)	93.9	N(1)- Pt(1)-Cl(1)	93.34	N(1)-Au(1)-Cl(1)	92.4(3)	93.7
N(5)-Pd(1)-Cl(1)	95.32(6)	93.9	N(5)- Pt(1)-Cl(1)	93.34	N(5)-Au(1)-Cl(1)	93.6(3)	93.7
C(1)-N(1)-C(8)	106.4(2)	106.9	C(1)-N(1)-C(7)	106.94	C(1)-N(1)-C(7)	108.6(9)	107.8
Pd(1)-N(1)-C(1)	130.24(17)	130.6	Pt(1)-N(1)-C(1)	130.64	Au(1)-N(1)-C(1)	130.9(7)	130.0
Pd(1)-N(1)-C(8)	123.27(18)	122.4	Pt(1)-N(1)-C(7)	122.27	Au(1)-N(1)-C(7)	120.4(7)	122.1
C(14)-N(5)-C(15)	105.6(2)	106.8	C(14)-N(5)-C(15)	106.94	C(14)-N(5)-C(15)	108.7(8)	107.8
Pd(1)-N(5)-C(14)	122.33(18)	122.4	Pt(1)-N(5)-C(14)	122.27	Au(1)-N(5)-C(14)	122.7(7)	122.1
Pd(1)-N(5)-C(15)	131.99(19)	130.7	Pt(1)-N(5)-C(15)	130.64	Au(1)-N(5)-C(15)	128.2(8)	130.0
N(3)-C(10)-N(4)	105.7(2)	105.7	N(3)-C(10)-N(4)	105.57	N(3)-C(10)-N(4)	107.5(10)	107.6
Pd(1)-C(10)-N(3)	126.7(2)	127.1	Pt(1)-C(10)-N(3)	127.22	Au(1)-C(10)-N(3)	127.9(8)	126.2
Pd(1)-C(10)-N(4)	127.54(19)	127.1	Pt(1)-C(10)-N(4)	127.22	Au(1)-C(10)-N(4)	124.5(8)	126.2

Note on crystal structure of complex 4: Following data reduction of complex 4 (CCDC 2379110), we determined that there are 38 electrons in the asymmetric unit, corresponding to 1.75 molecules of acetonitrile. It is not uncommon for metal complexes to exhibit multiple coordination modes or slight positional variations, particularly in the presence of positional or occupational disorder. In the present structure, one of the $AuCl_2$ units has site occupancy of 0.5. Additionally, due to the strong X-ray scattering of heavy atoms such as gold, any discrepancies in anisotropic displacement parameters (ADPs) are more pronounced. These factors likely contribute to the observed residual electron density around the gold atom, which in turn affects the refinement of the Au center in the complex. A depiction of the residual electron density map for complex 4 is provided below.

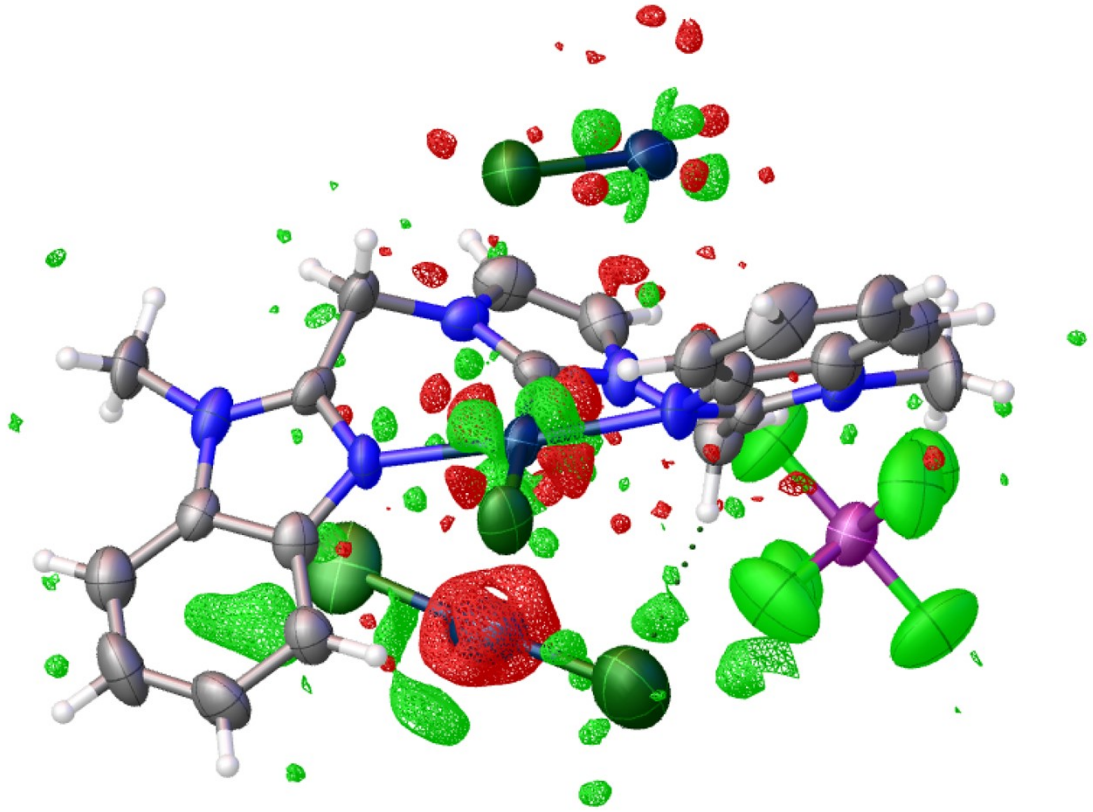

Note on crystal structure of complex 2: In the crystal structure of complex 2 we found that there is a mixture of Et_2O and two different MeCN positions. However, due to the electron density observed, we were only able to model one MeCN molecule with occupancy of 0.25 and one Et_2O molecule with occupancy of 0.75. Additionally, the PF_6^- counter ion has been modelled in two different positions with occupancies of 0.75 and 0.25, respectively. Moreover, RIGU and ISOR restraints were applied as needed throughout the refinement.

Table S4 Compositions (in %) of selected molecular orbitals for complexes **2**, **3** and **4** computed using B3LYP-D3/ def2-TZVP (Au, Pd), 6-31G** (H, C, N, Cl) level of theory.

MOs	Complex **2**					Complex **3**					Complex **4**				
	% of composition					% of composition					% of composition				
	Pd	**Cl**	**L1**	**L2**	**L3**	**Pt**	**Cl**	**L1**	**L2**	**L3**	**Au**	**Cl**	**L1**	**L2**	**L3**
LUMO+3	10	0	44	23	23	52	9	15	12	12	2	0	27	35	35
LUMO+2	3	0	12	43	42	14	1	50	18	18	2	0	13	43	42
LUMO+1	12	1	36	25	26	2	0	11	43	43	1	60	11	11	
LUMO	50	11	16	11	11	11	1	26	31	31	38	14	17	15	15
HOMO	9	56	1	17	17	17	49	5	14	14	1	4	0	48	48
HOMO-1	16	78	4	1	1	23	64	7	3	3	1	0	0	50	49
HOMO-2	6	1	0	46	46	15	1	0	42	42	0	0	2	49	49
HOMO-3	1	12	2	42	44	1	7	2	45	45	0	0	2	49	49

[a] Where L1 = Imidazole and L2, L3 = Benzimidazole.

Table S5 Vertical electronic transition as computed at TD-DFT $SMD_{(acetonitrile)}$ B3LYP-D3/def2-TZVP (Pd), 6-31G** (C, H, N, Cl) level of theory for complex **2**.

E_e (eV)	λ_{theo} (nm)	Osc. Strength (*f*)	Key transitions
3.5676	347.53	0.0073	HOMO→LUMO
3.8012	326.17	0.0145	HOMO-2→LUMO
4.6740	265.27	0.0192	HOMO→LUMO+1
4.7391	261.62	0.1092	HOMO→LUMO+2
4.7537	260.82	0.0968	HOMO-1→LUMO+1
4.8725	254.46	0.0141	HOMO-7→LUMO
4.9192	252.04	0.0763	HOMO-2→LUMO+1
4.9505	250.45	0.1489	HOMO-4→LUMO+1
4.9756	249.19	0.0863	HOMO-3→LUMO+1
5.1314	241.62	0.0205	HOMO→LUMO+3

Table S6 Vertical electronic transition as computed at TD-DFT $SMD_{(acetonitrile)}$ B3LYP-D3/def2-TZVP (Pt), 6-31G** (C, H, N, Cl) level of theory for complex **3**.

E_e (eV)	λ_{theo} (nm)	Osc. Strength (*f*)	Key transitions
4.3954	282.08	0.0293	HOMO→LUMO
4.4104	281.11	0.0120	HOMO→LUMO+3
4.5527	272.33	0.2190	HOMO-1→LUMO
4.6888	264.43	0.0220	HOMO-2→LUMO+3
4.8379	256.28	0.0126	HOMO-2→LUMO
4.8626	254.98	0.0464	HOMO-5→LUMO
4.9301	251.49	0.1570	HOMO-3→LUMO+1
4.9705	249.44	0.1464	HOMO→LUMO+2
5.0139	247.28	0.0448	HOMO-1→LUMO+2
5.1407	241.18	0.0359	HOMO-6→LUMO
5.1736	239.65	0.0925	HOMO-2→LUMO+2

Table S7 Vertical electronic transition as computed at TD-DFT $SMD_{(acetonitrile)}$ B3LYP-D3/def2-TZVP (Au), 6-31G** (C, H, N,Cl) level of theory for complex **4**.

E_e (eV)	λ_{theo} (nm)	Osc. Strength (*f*)	Key transitions
3.0023	412.96	0.0061	HOMO-1→LUMO
3.8788	319.65	0.0179	HOMO-5→LUMO
4.0639	305.08	0.0084	HOMO-6→LUMO
4.7093	263.28	0.1372	HOMO→LUMO+1
4.8581	255.21	0.2202	HOMO-3→LUMO+1
4.8635	254.93	0.0504	HOMO-4→LUMO+1
4.9401	250.97	0.0261	HOMO-5→LUMO+2
4.9559	250.17	0.0337	HOMO→LUMO+2
5.0255	246.71	0.0887	HOMO-4→LUMO+2
5.0322	246.38	0.0196	HOMO-3→LUMO+2
5.0378	246.11	0.0120	HOMO-8→LUMO
5.1528	240.62	0.0266	HOMO-12→LUMO
5.2304	237.05	0.0173	HOMO→LUMO+3

Table S8 Summary of binding affinities, types of interactions, the active amino acids and the corresponding bond distances obtained from *in silico* investigations of synthesized complexes (**2**, **3**, and **4**) with TrxR1 (PDB ID: 2J3N).

Receptor–ligand	**Binding affinity (kcal/mol)**	**Types of interaction**	**Interacting AA chain; AA name; AA no.;**	**Bond distance (Å)**	**Pictorial view**
Human Thioredoxin Reductase 1-Complex **2**	-7.95	Carbon-hydrogen bond	E:Asn419	1.78	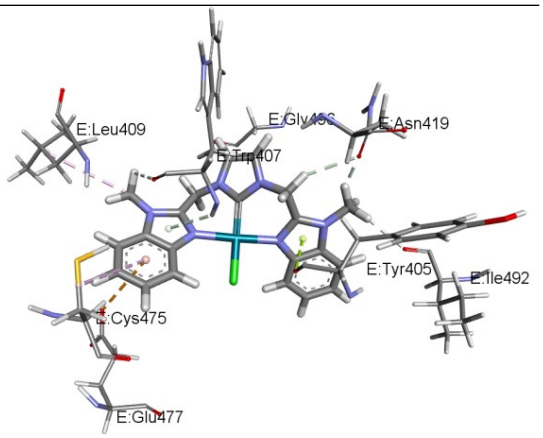
			E:Ile492	2.25	
			E:Gly496	2.53	
			E:Asn419	2.62	
			E:Trp407	2.97	
		Pi-donor interaction	E:Trp407	2.96	
		Pi-lone pair interaction	E:Tyr405	2.93	
		Pi-anion interaction	E:Glu477	4.21	
		Pi-alkyl interaction	E:Cys475	5.17	
		Alkyl-alkyl interaction	E:Leu409	4.34	
Human Thioredoxin Reductase 1-Complex **3**	-7.21	Pi-donor interaction	F:Gln72	2.63	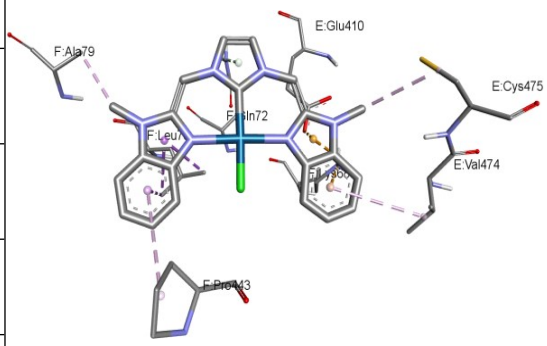
		Pi-donor; pi-cation interaction	F:Lys68	2.84	
		Pi-cation interaction	F:Lys68	3.52	
		Pi-anion interaction	E:Glu410	3.18	
		Pi-sigma interaction	F:Leu75	3.25	
				3.66	
				3.59	
		Pi-alkyl interaction	F:Pro443	5.26	
		Alkyl-alkyl interaction	F:Ala79	3.71	
			E:Cys475	3.76	

Human Thioredoxin Reductase 1-Complex **4**	-8.70	Carbon-hydrogen bond	F:Tyr116	2.87	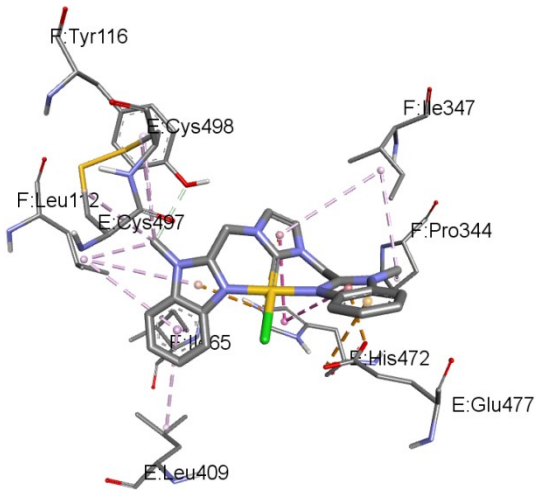
		Pi-cation interaction	E:His472	4.03	
				4.30	
			E:Glu477	4.20	
		Pi-anion interaction	E:Glu477	3.03	
				4.20	
		Pi-pi stacked interaction	E:His472	4.36	
				5.05	
		Pi-alkyl interaction	F:Tyr116	4.59	
			E:Leu409	4.91	
			F:Ile347	5.30	
			F:Leu112	5.34	
				5.47	
		Alkyl-alkyl interaction	F:Pro344	4.17	
			F:Ile347	4.55	
			E:Cys497	4.51	
			E:Cys498	4.88	

Table S9 The physicochemical characteristics of complexes derived from the SwissADME database.

Complex	nHA	nAHA	F.Csp^3	nRB	nHBA	nHBD	MR	TPSA (Å^2)
2	29	18	0.24	0	0	0	120.06	26.20
3	29	18	0.24	0	0	0	120.06	26.20
4	29	18	0.24	0	0	0	120.06	26.20

Table S10 Summary of lipophilicity and water solubility criteria for the complexes derived from the SwissADME database.

Complex	Lipophilicity	Water solubility					
	Consensus Log $P_{O/W}$	Log *S* (ESOL)	Solubility class	Log *S* (Ali)	Solubility class	Log *S* (SILICOS-IT)	Solubility class
2	1.37	-5.85	Moderately soluble	-4.15	Moderately soluble	-3.51	Soluble
3	1.48	-6.40	Poorly soluble	-4.15	Moderately soluble	-3.71	Soluble
4	1.48	-6.41	Poorly soluble	-4.15	Moderately soluble	-3.71	Soluble

Table S11 The pharmacokinetic characteristics of complexes derived from the SwissADME database.

Complex	GI absorption	BBB permeant	P-gp substrate	Bioavailability score
2	High	Yes	Yes	0.55
3	High	Yes	Yes	0.55
4	High	Yes	Yes	0.55

Table S12 Drug-likeness characteristics of complexes derived from the SwissADME database.

Complex	Lipinski	Ghose	Veber	Egan	Muegge	PAINS
2	Yes	No	Yes	Yes	Yes	0 alert
3	Yes	No	Yes	Yes	Yes	0 alert
4	Yes	No	Yes	Yes	Yes	0 alert

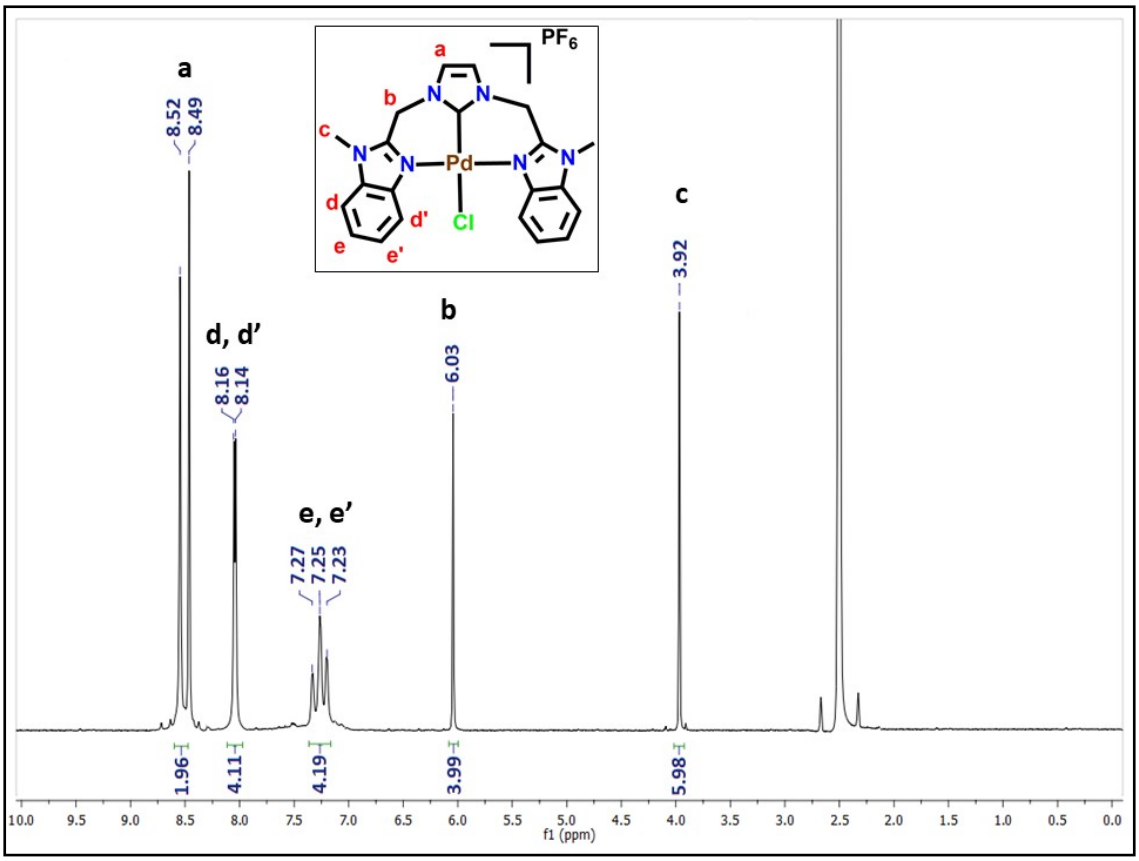

Figure S1 ^{1}H NMR spectra of complex **2**.

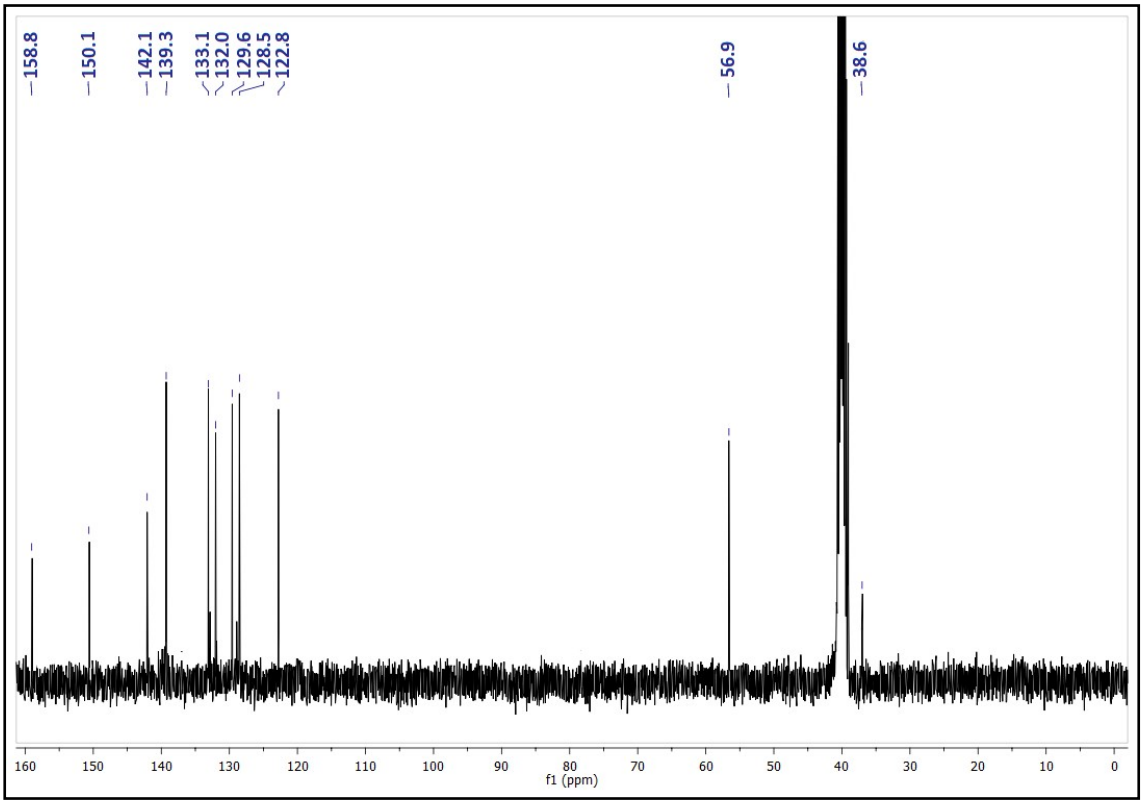

Figure S2 ^{13}C NMR spectra of complex **2**.

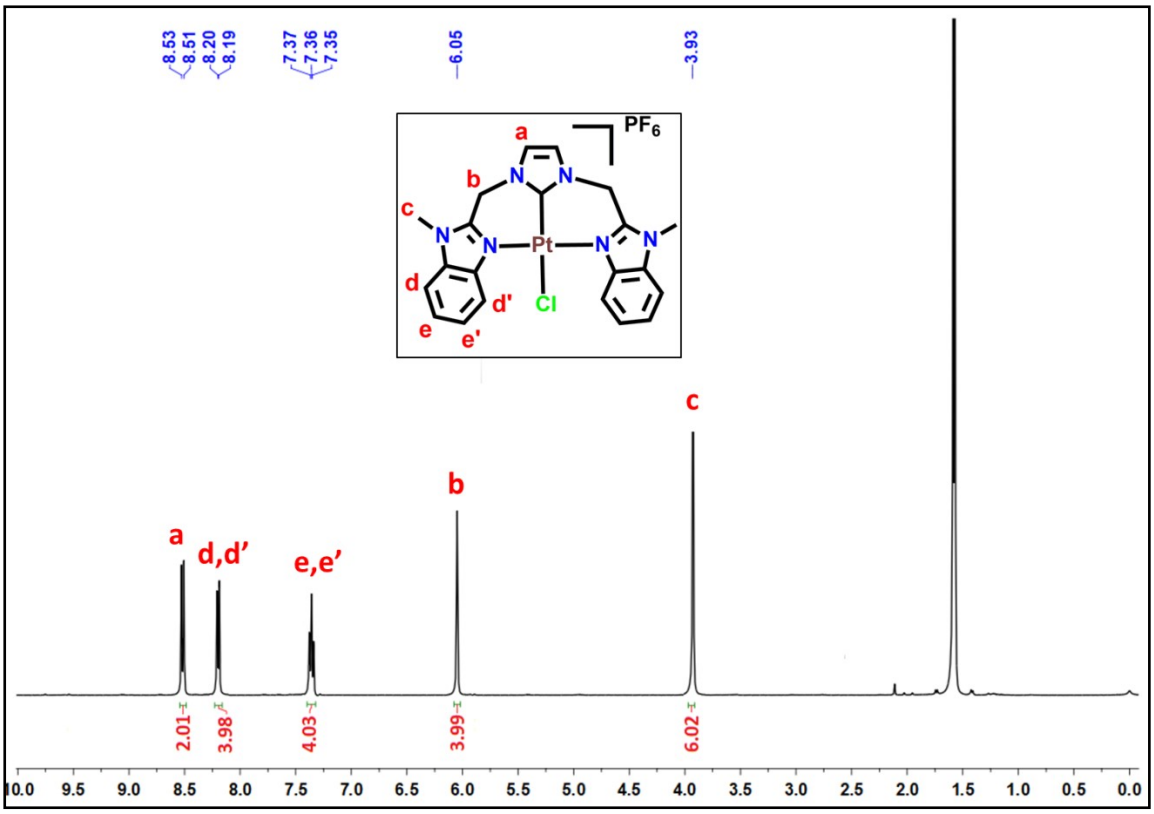

Figure S3 ^{1}H NMR spectra of complex **3**.

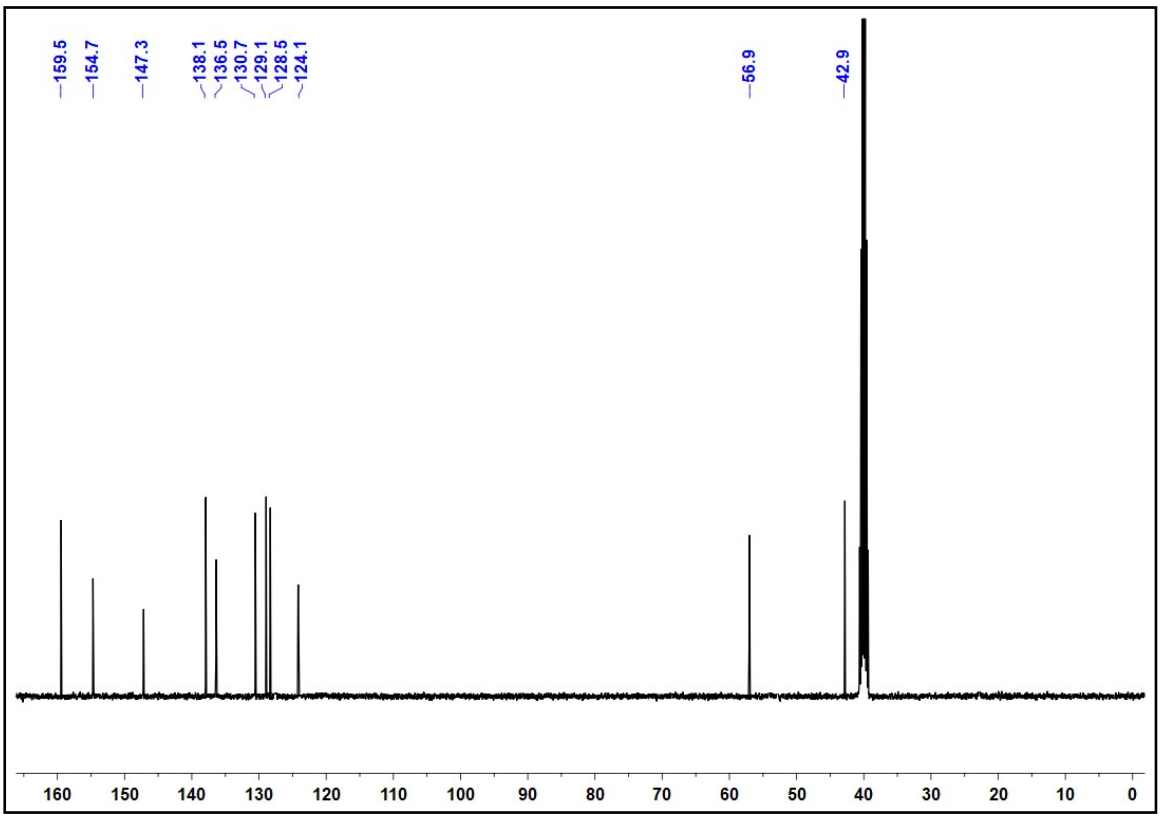

Figure S4 ^{13}C NMR spectra of complex **3**.

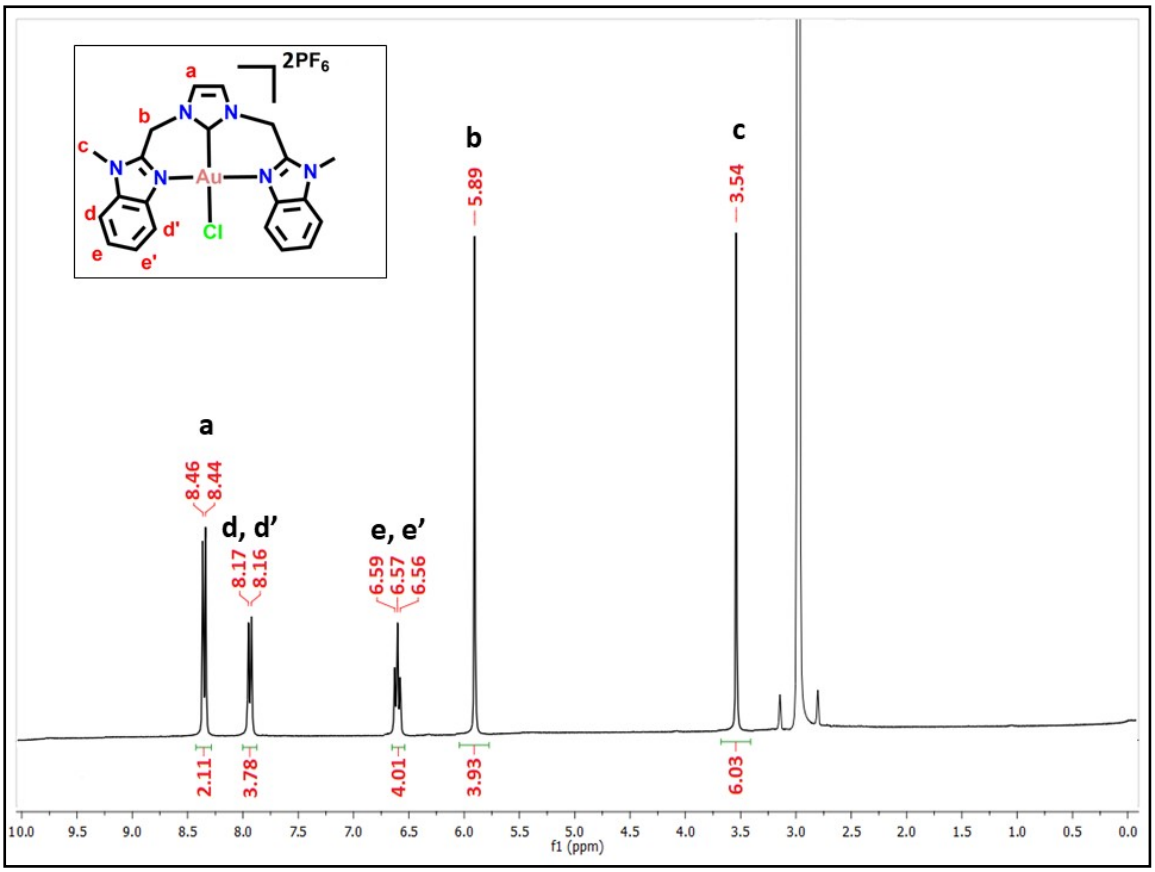

Figure S5 ^{1}H NMR spectra of complex **4**.

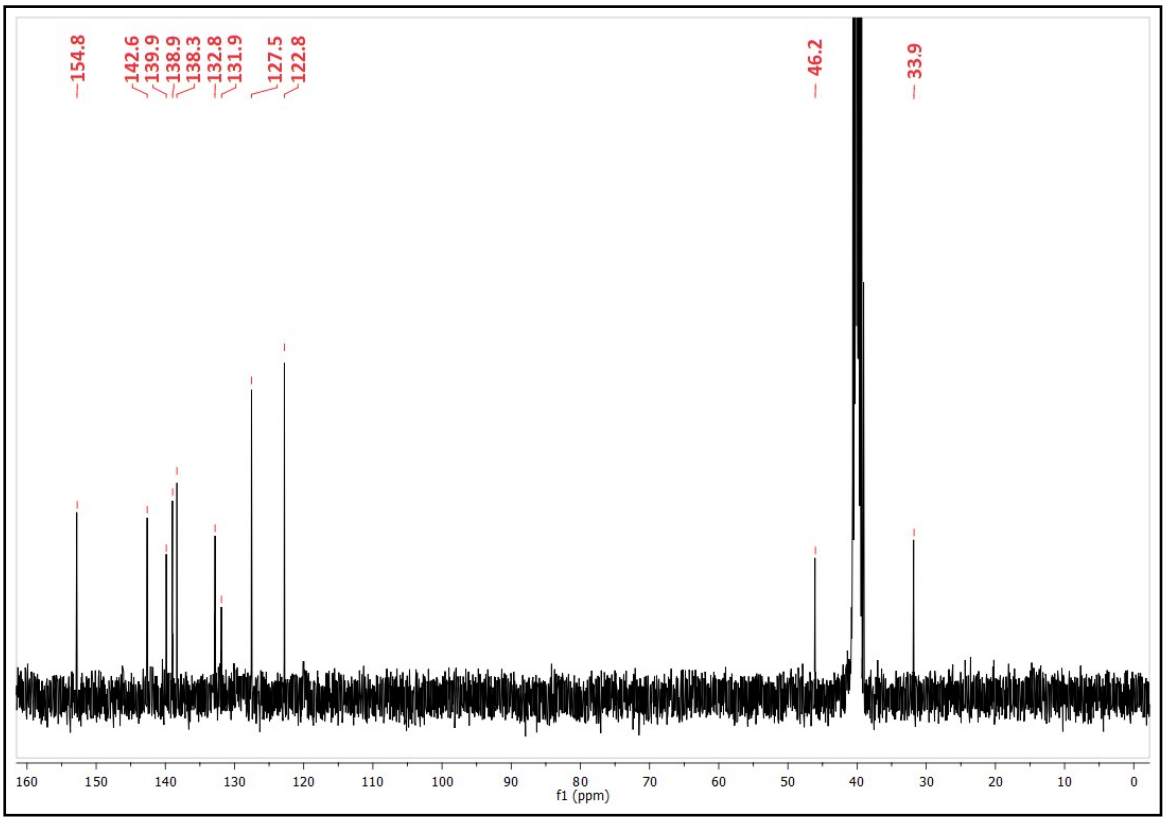

Figure S6 ^{13}C NMR spectra of complex **4**.

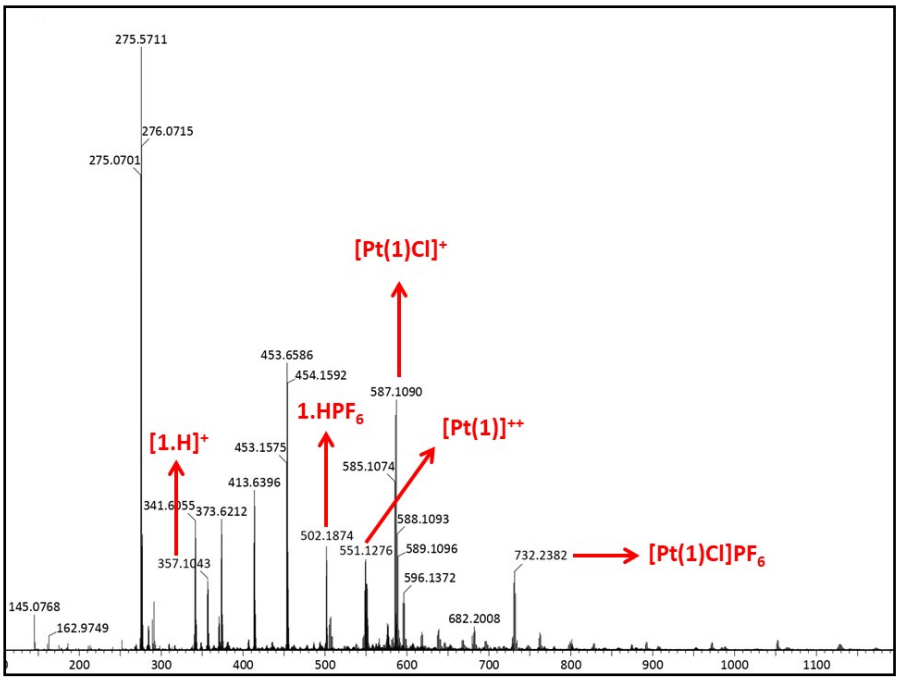

Figure S7 HR-MS spectra of complex **3**.

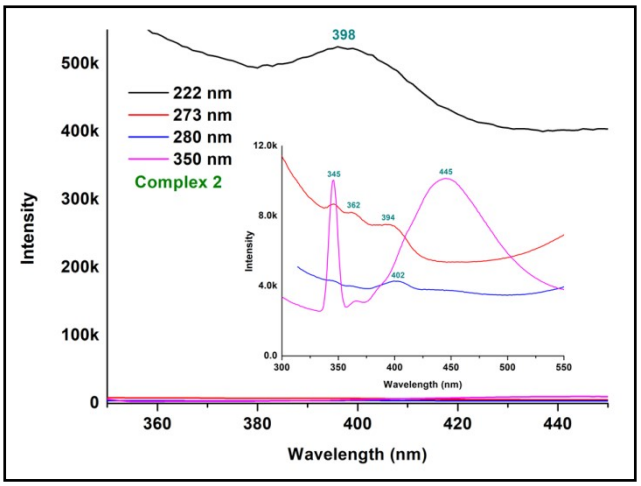

Figure S8 Emission spectra of complex **2** at different excitation wavelengths (222, 273, 280, and 350 nm) recorded in acetonitrile at room temperature.

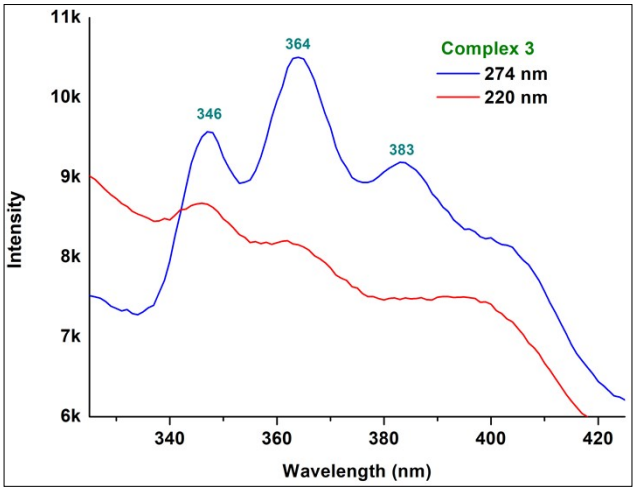

Figure S9 Emission spectra of complex **3** at different excitation wavelengths (220 and 274 nm) recorded in acetonitrile at room temperature.

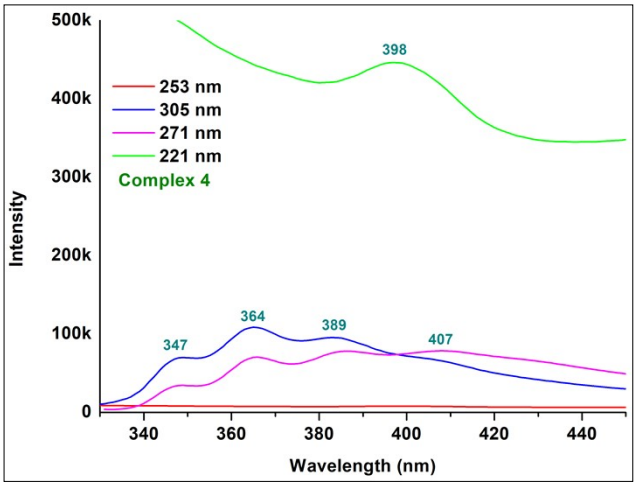

Figure S10 Emission spectra of complex **4** at different excitation wavelengths (221, 253, 271, and 274 nm) recorded in acetonitrile at room temperature.

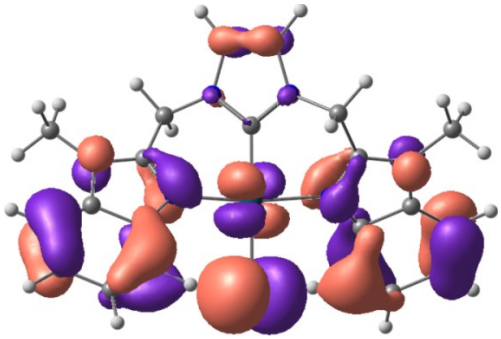

HOMO (E= -6.3485 eV)

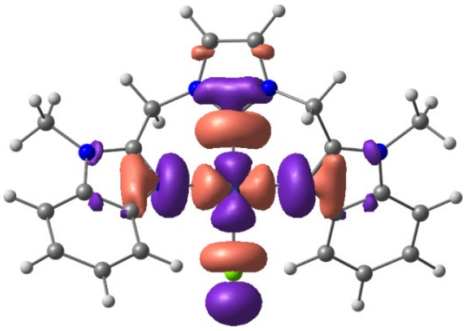

LUMO (E= -1.4525 eV)

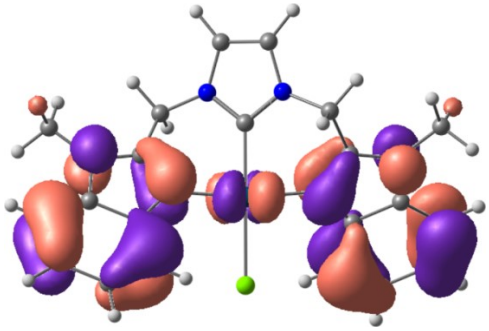

HOMO-1 (E= -6.3784 eV)

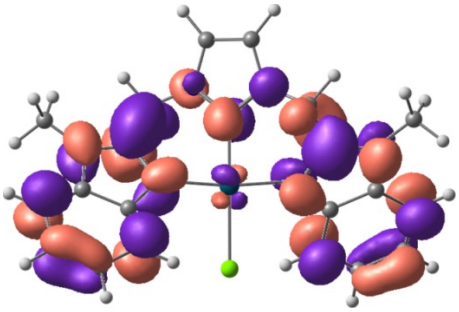

LUMO+1 (E= -1.0542 eV)

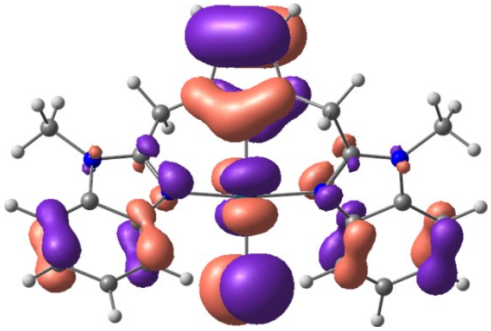

HOMO-2 (E= -6.5327 eV)

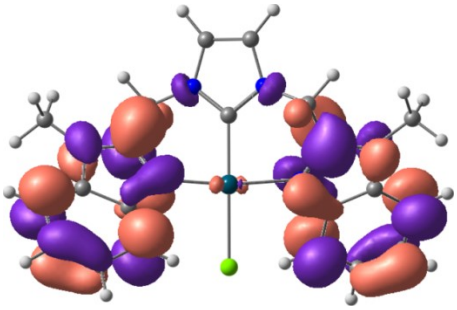

LUMO+2 (E= -0.9948 eV)

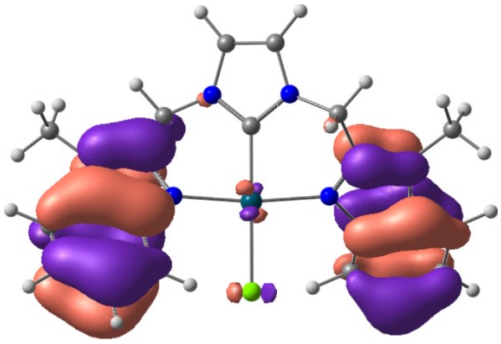

HOMO-3 (E= -6.6219 eV)

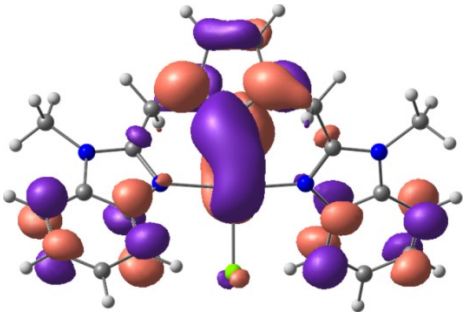

LUMO+3 (E= -0.5377 eV)

Figure S11 Molecular orbitals obtained for complex **2** at TD-DFT $SMD_{(acetonitrile)}$ / B3LYP-D3/def2-TZVP (Pd), 6-31G** (C, H, N, Cl) level of theory.

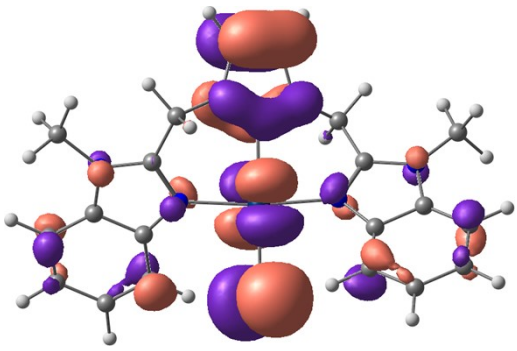

HOMO (E=-6.1895 eV)

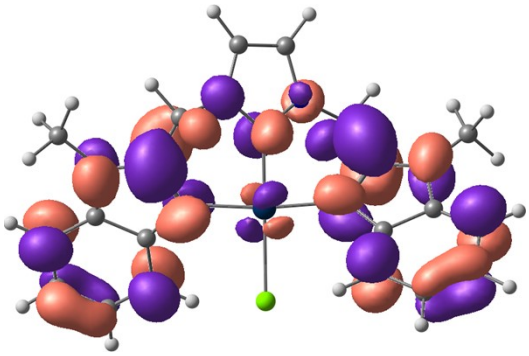

LUMO (E=-1.1173 eV)

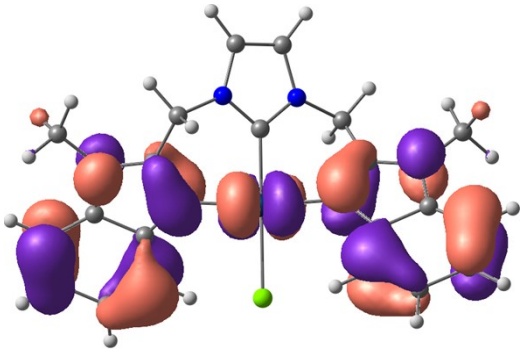

HOMO-1 (E=-6.2997 eV)

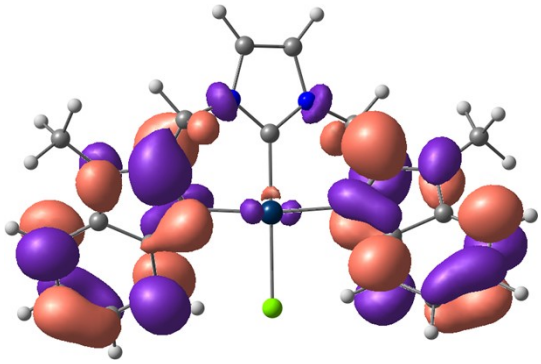

LUMO+1 (E=-1.0408 eV)

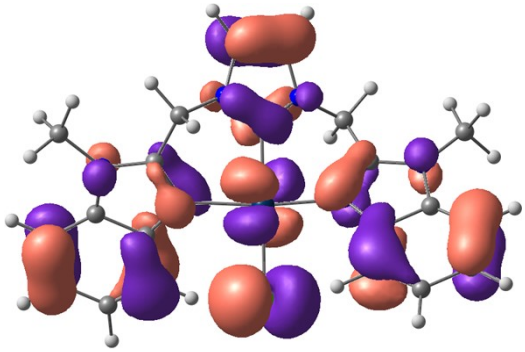

HOMO-2 (E=-6.4279 eV)

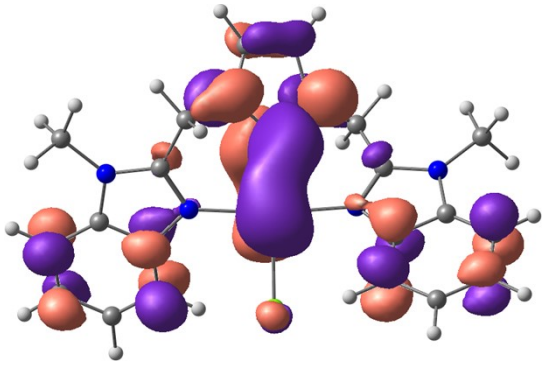

LUMO+2 (E=-0.5706 eV)

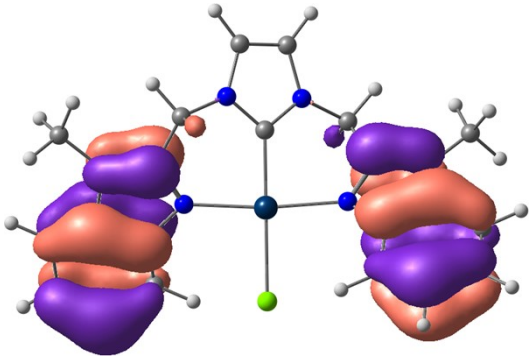

HOMO-3 (E=-6.6625 eV)

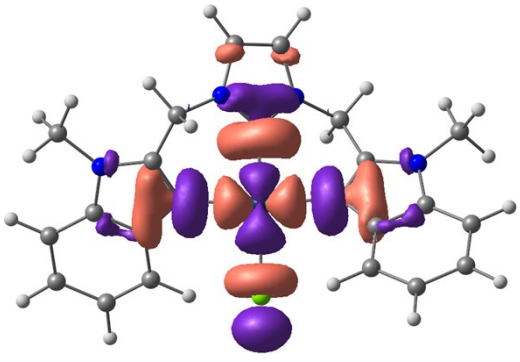

LUMO+3 (E=-0.4144 eV)

Figure S12 Molecular orbitals obtained for complex **3** at TD-DFT $SMD_{(acetonitrile)}$ / B3LYP-D3/def2-TZVP (Pd), 6-31G** (C, H, N, Cl) level of theory.

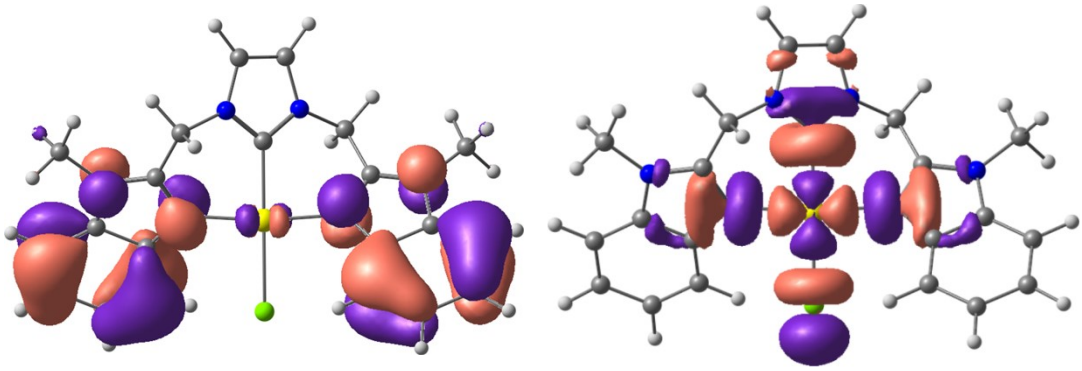

HOMO (E=-6.8609 eV) **LUMO** (E=-3.1010 eV)

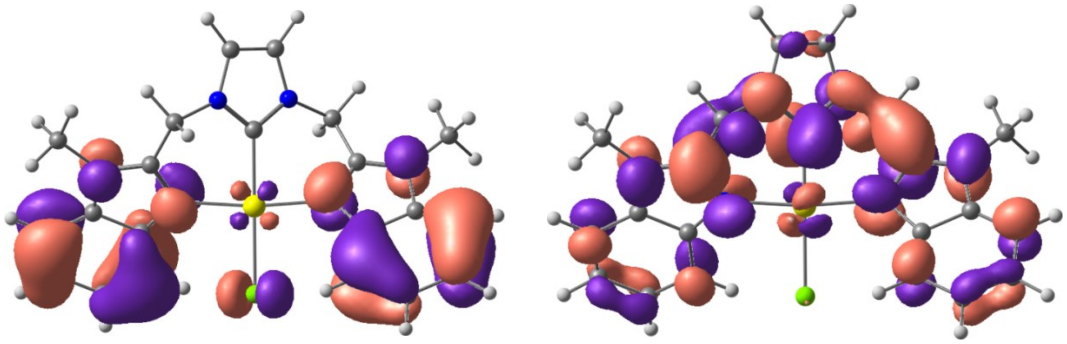

HOMO-1 (E=-6.8671 eV) **LUMO+1** (E=-1.5976 eV)

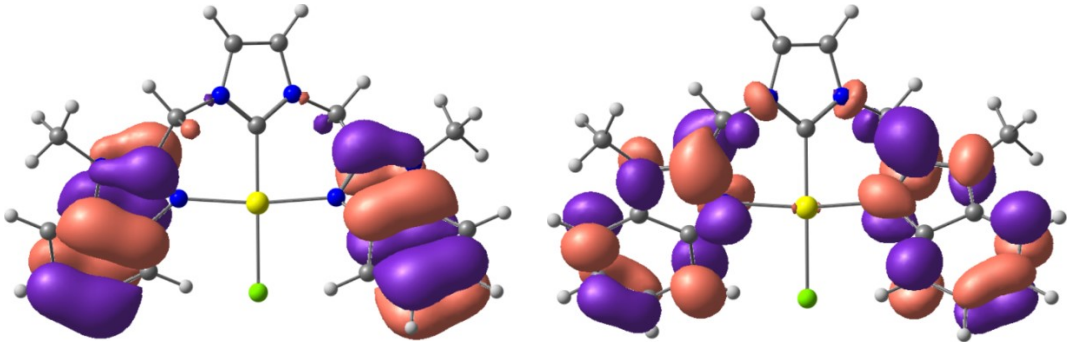

HOMO-2 (E=-6.9972 eV) **LUMO+2** (E=-1.4604 eV)

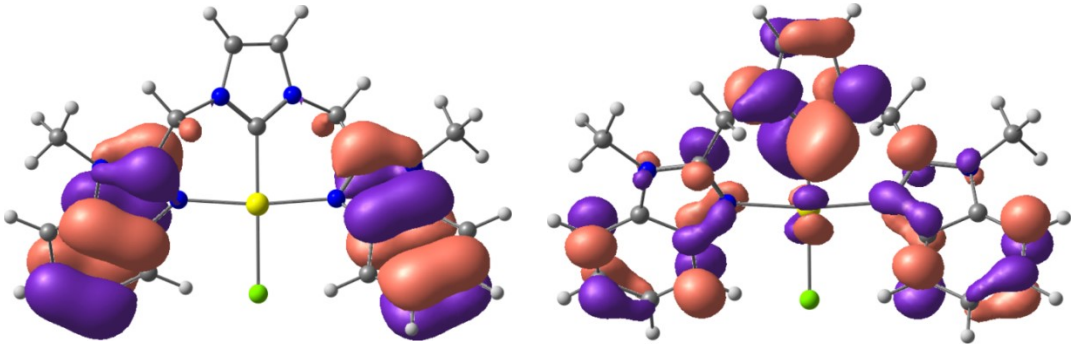

HOMO-3 (E=-7.0051 eV) **LUMO+3** (E=-1.1187 eV)

Figure S13 Molecular orbitals obtained for complex **4** at TD-DFT $SMD_{(acetonitrile)}$ / B3LYP-D3/def2-TZVP (Pd), 6-31G** (C, H, N, Cl) level of theory.

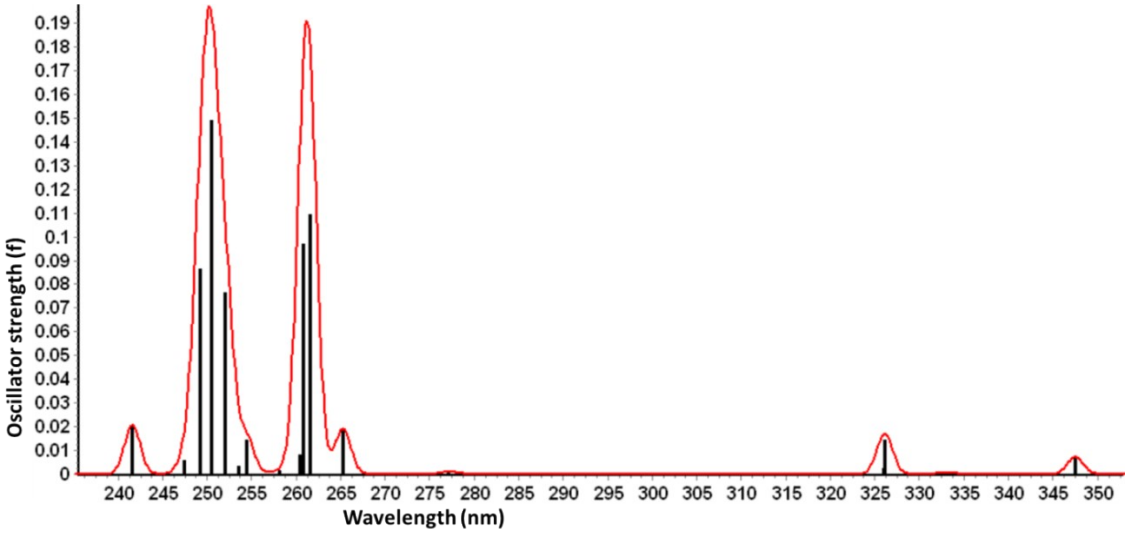

Figure S14 Simulated absorption spectra of complex **2** in CH_3CN media using TDDFT.

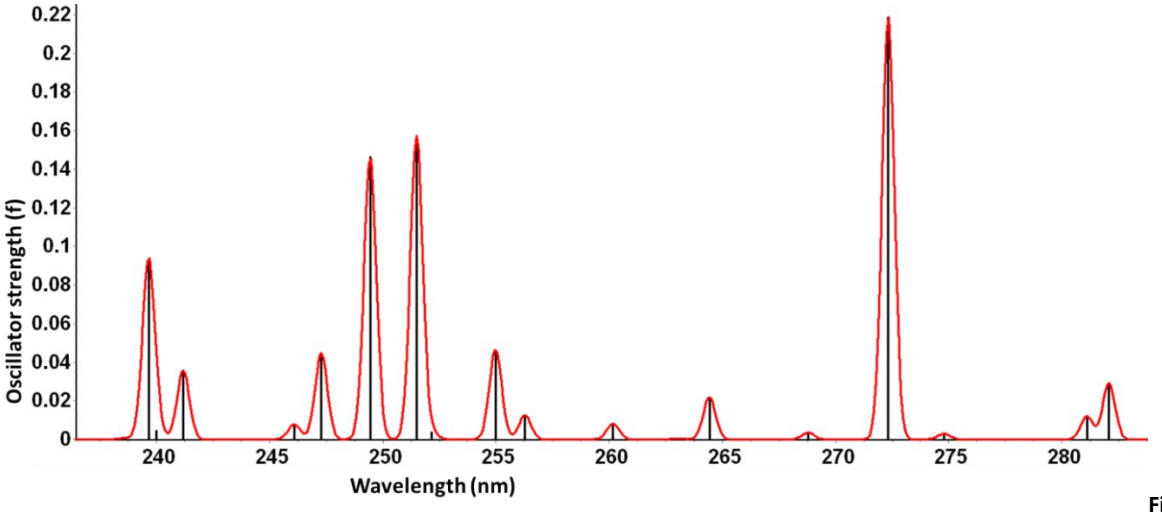

Figure S15 Simulated absorption spectra of complex **3** in CH_3CN media using TDDFT.

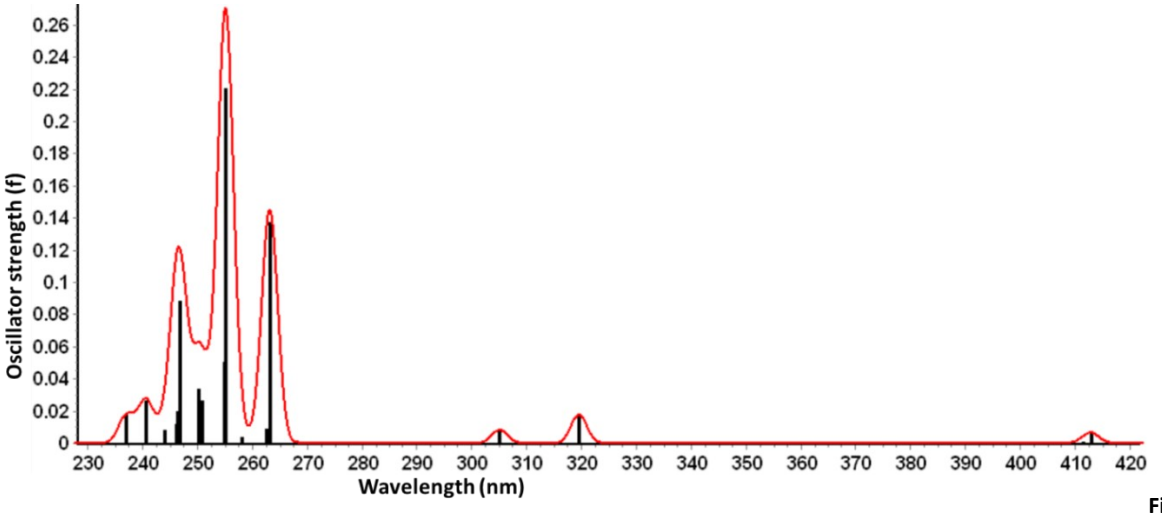

Figure S16 Simulated absorption spectra of complex **4** in CH_3CN media using TDDFT.

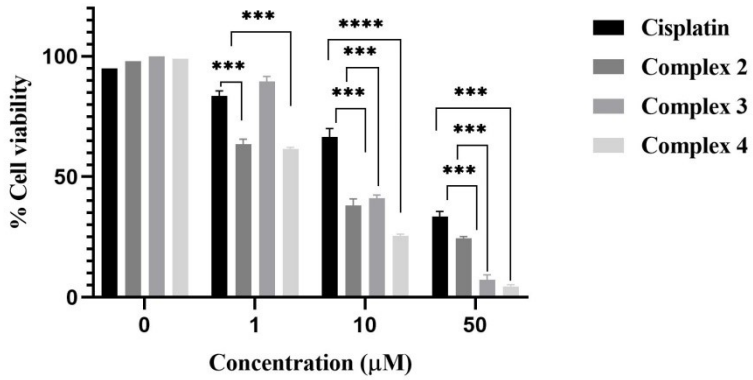

Figure S17 Comparison of cell viability assay among cisplatin and complexes **2**, **3**, and **4** in MDA-MB 231 cells.

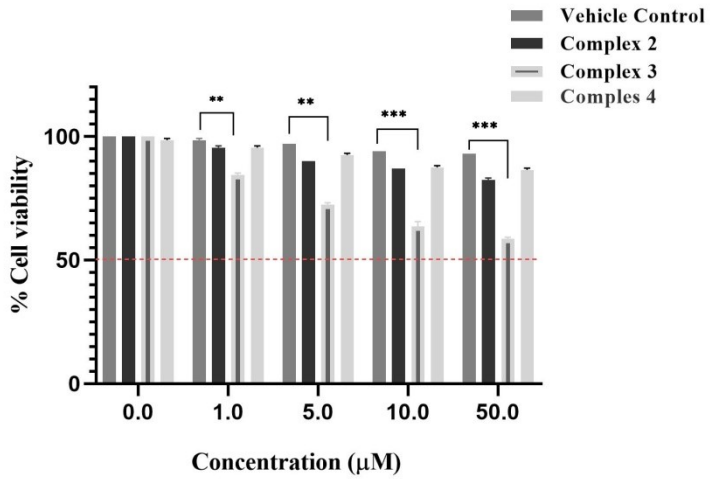

Figure S18 Cytotoxicity assay of complexes **2**, **3**, and **4** in healthy cells (Plasma Blood Mononuclear Cells isolated from healthy individuals).

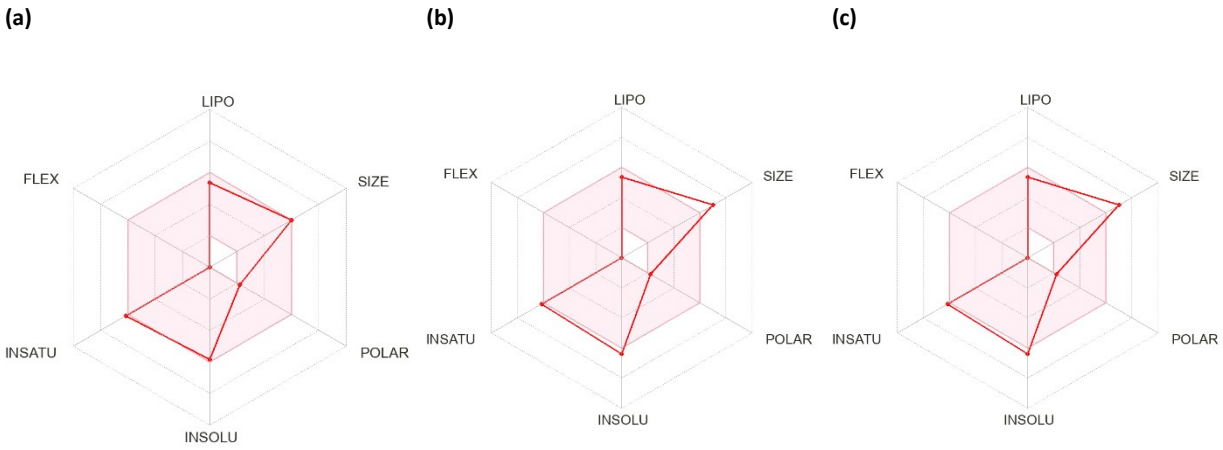

Figure S19 Radar charts of complexes **2** (a), **3** (b), and **4** (c) depicting their physicochemical characteristics.

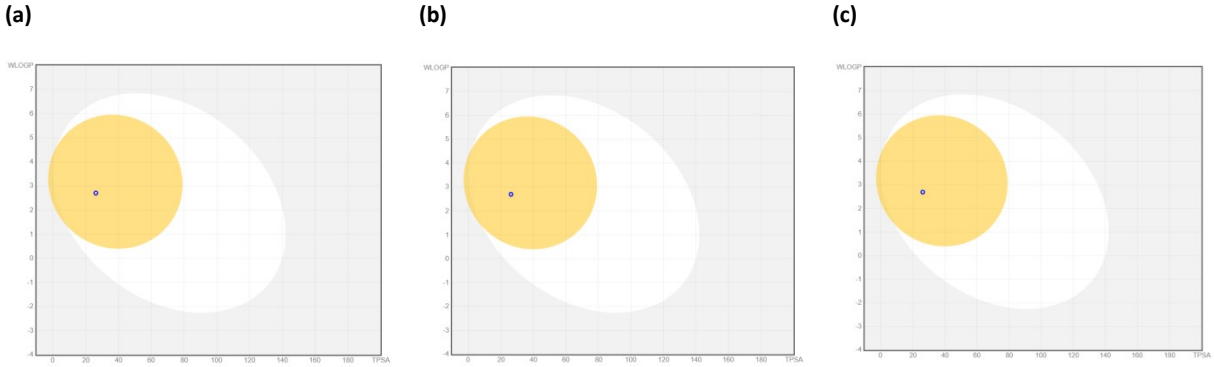

Figure S20 Boiled-egg representations of complexes **2** (a), **3** (b), and **4** (c) implying that complexes can be effluated from the central nervous system as substrates for P-glycoprotein.